Since January 2020 Elsevier has created a COVID-19 resource centre with free information in English and Mandarin on the novel coronavirus COVID-19. The COVID-19 resource centre is hosted on Elsevier Connect, the company's public news and information website.

Analytica Chimica Acta 1200 (2022) 339590

Contents lists available at ScienceDirect

Analytica Chimica Acta

journal homepage: www.elsevier.com/locate/aca

A point-of-care SARS-CoV-2 test based on reverse transcription loop-mediated isothermal amplification without RNA extraction with diagnostic performance same as RT-PCR

Nelson Odiwuor [a, b, c], Jin Xiong [a], Faith Ogolla [a, b, c], Wei Hong [a, b], Xiaohong Li [a], Fazal Mehmood Khan [a, b], Nuo Wang [a], Junping Yu [a], Hongping Wei [a, b, c, *]

[a] CAS Key Laboratory of Special Pathogens and Biosafety, Centre for Biosafety Mega-Science, Wuhan Institute of Virology, Chinese Academy of Sciences, Wuhan, 430071, China
[b] University of Chinese Academy of Sciences, Beijing, 100049, China
[c] Sino-Africa Joint Research Centre, Nairobi, 62000 - 00200, Kenya

HIGHLIGHTS

- The direct RT-LAMP assay developed is simple and extraction-free, requiring only heating and bead-assisted mechanical lysis for sample preparation.
- A calibrated template transfer tool was devised to simplify sample addition into RT-LAMP reactions.
- The assay is rapid and has a high diagnostic performance of 99.30% accuracy, 98.81% sensitivity, and 100% selectivity compared to RT-PCR.

GRAPHICAL ABSTRACT

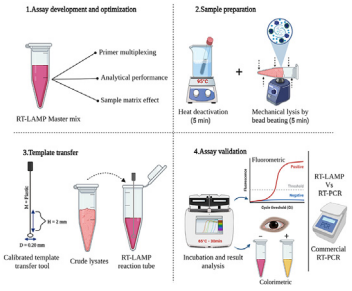

ARTICLE INFO

Article history:
Received 21 May 2021
Received in revised form
3 February 2022
Accepted 7 February 2022
Available online 15 February 2022

Keywords:
RT-LAMP
Point-of-care
COVID-19
SARS-CoV-2
Rapid testing
Bead beating

ABSTRACT

The global public health crisis and economic losses resulting from the current novel coronavirus disease (COVID-19) pandemic have been dire. The most used real-time reverse transcription polymerase chain reaction (RT-PCR) method needs expensive equipment, technical expertise, and a long turnaround time. Therefore, there is a need for a rapid, accurate, and alternative technique of diagnosis that is deployable at resource-poor settings like point-of-care. This study combines heat deactivation and a novel mechanical lysis method by bead beating for quick and simple sample preparation. Then, using an optimized reverse transcription loop-mediated isothermal amplification (RT-LAMP) assay to target genes encoding the open reading frame 8 (*ORF8*), spike and nucleocapsid proteins of the novel coronavirus, SARS-CoV-2. The test results can be read simultaneously in fluorometric and colorimetric readouts within 40 min from sample collection. We also calibrated a template transfer tool to simplify sample addition into LAMP reactions when pipetting skills are needed. Most importantly, validation of the direct RT-LAMP system based on multiplexing primers S1:ORF8 in a ratio (1:0.8) using 143 patients' nasopharyngeal swab samples showed a diagnostic performance of 99.30% accuracy, with 98.81% sensitivity and 100% selectivity, compared to commercial RT-PCR kits. Since our workflow does not rely on RNA extraction and purification, the time-to-result is two times faster than other workflows with FDA emergency use

* Corresponding author. No.44, Wuhan, Hubei, 430071, China.
E-mail address: hpwei@wh.iov.cn (H. Wei).

https://doi.org/10.1016/j.aca.2022.339590

authorization. Considering all its strengths: speed, simplicity, accuracy and extraction-free, the system can be useful for optimal point-of-care testing of COVID-19.

1. Introduction

Diagnosis constitutes a vital part of guiding epidemiological strategies and public health interventions in controlling the novel coronavirus disease (COVID-19) outbreak. Moreover, in the absence of effective drugs and inequitable access to vaccines against the virus, the importance of wide-scale and targeted testing cannot be overstated. Currently, real-time reverse transcription polymerase chain reaction (RT-PCR) is the reference method for diagnosing COVID-19 [1]. The nucleic acid testing technique is preferred since it can accurately detect etiological disease agents based on their unique molecular sequences. Rapid serological tests are complementary methods of detection, often used at point-of-care (POC). Their strengths lie in detecting past infections and people with developed immunity, which could provide an overall picture of the pandemic. However, antibody-based tests do not detect early infections because of late seroconversion time post-exposure. Besides, rapid antigen tests have reported lower sensitivity than molecular tests [2]. Despite the apparent advantages of RT-PCR, the method is sophisticated and requires expensive equipment, skilled labor, and a long turnaround time, making it difficult to scale its operations at POC where they are needed most. Apart from the technologies mentioned above, there have been several attempts to develop point-of-care SARS-CoV-2 biosensors based on nanomaterials, field-effect transistors, surface plasmon resonance, chemiluminescence, electrochemistry, and CRISPR/CAS systems coupled with or without isothermal nucleic acid amplification technologies (INAAT) such as recombinase polymerase amplification (RPA) and loop-mediated isothermal amplification (LAMP) [3–9]. Although the novel biosensors developed are promising, their design and optimizations are complex, cost-prohibitive, and time-consuming. For example,electrochemical-based biosensors need calibration and electrode replacement regularly to function optimally, limiting their applicability at the POC. Also, lateral flow devices are sometimes affected by sample matrix; hence appropriate sample pretreatment is necessary [10,11].

Sample preparation is a key challenge for deploying existing technologies to the field [12]. The conventional way to prepare samples for nucleic acid amplification tests (NAATs) involves cell lysis or nucleic acid extraction and purification in centralized laboratories using commercial kits on benchtop equipment. Generally, the commercial nucleic acid processes involve silica membrane-based spin columns, consumables such as pipette tips and centrifuge tubes, several buffers for cell lysis, column washing, and sample elution. Although commercially available kits such as NucliSens easyMAG (bioMérieux) and QIAmp DNA/RNA purification kit (Qiagen) can rapidly prepare samples, they cannot be deployed at the POC. Due to high demand and logistical challenges, their supply and availability were constrained during the pandemic. Essentially, cell lysis is the most crucial step for solid-phase extraction methods; hence the most appropriate lysis technique should be selected depending on the sample type [13]. There is a concern that RNA may not be extracted efficiently from complex clinical samples using commercial kits, particularly those that rely solely on lysis buffer or enzymatic lysis for initial sample processing. Incomplete sample lysis may lead to blockage of column-based extraction methods, resulting in poor elution. This problem could lead to sample loss in weakly positive samples. Taken together, there is a need to develop rapid and reliable diagnostic tools for use at POC rather than centralized laboratories in order to keep up with the demand for mass testing.

LAMP, initially developed by Notomi et al., is often used as a molecular diagnostics alternative to PCR [14]. The method is specific, sensitive, and rapid and can tolerate unpurified sample input. It can also be performed under isothermal conditions due to the high strand-displacement activity of the *Bst* DNA polymerase enzyme. LAMP is an ideal method of choice in the field. Previously, combined with reverse transcription steps (RT-LAMP), it was used to detect RNA viruses, including influenza viruses, middle east respiratory syndrome (MERS-CoV), SARS-CoV, and even SARS-CoV-2 [15–18]. Although many studies reported using RT-LAMP for SARS-CoV-2 detection, diagnostic performance was lower than RT-PCR, especially without RNA extraction [19,20]. Moreover, non-specific amplification frequently observed when using LAMP is a significant drawback in deploying the technology as a mature clinical diagnostic tool. Previous investigations have reported that false-positive reactions could occur due to carry-over contamination, primer hybridization between multiple primer sets, and the type of *Bst* polymerase enzyme or reaction buffers used [21]. To overcome the above challenges, uracil-DNA-glycosylase (UDG)-LAMP, probe-based methods with proofreading enzymes, and additives such as pullulan and dimethyl sulfoxide (DMSO) have been proposed [22–24]. However, these approaches do not eliminate or inform on the nature of non-specific amplification in LAMP reactions. Therefore, it is desirable to account for false-positive reactions using a reliable method that may subsequently aid in tuning reaction conditions.

Herein, we developed a quick and efficient sample mechanical lysis method, avoiding the bottlenecks associated with RNA extraction. Building on our preliminary work [25], we designed primer sets with higher sensitivity and performed optimizations involving high resolution melting curve analysis and primer multiplexing. We also calibrated a template transfer tool that may simplify template addition into LAMP reactions. As a result, a robust RT-LAMP assay was successfully established with diagnostic performance same as RT-PCR without RNA extraction, which could facilitate the diagnosis of COVID-19 at resource-limited settings.

2. Materials and methods

2.1. Sample collection and processing

Nasopharyngeal swabs were collected from patients suspected of COVID-19 from various designated hospitals in Wuhan, China, on the 12th of March 2020, and sent to Wuhan Institute of Virology (WIV), CAS, by China CDC. The samples were then processed in a biosafety level 2 laboratory, WIV. Of note, the patient specimens were transported and stored in a viral transport medium (VTM; Yocon Biology, Beijing, China) at 4 °C. 1x Phosphate-buffered saline (PBS) and saliva samples from healthy volunteers were spiked with cell culture supernatant of SARS-CoV-2 grown on Vero E6 cells in a biosafety level 3 lab, then serially diluted in their respective media in a ten-fold dilution series. All the samples were deactivated by heat at 95 °C for 5 min on a thermostatic water bath. Deactivation of

SARS-CoV-2 at similar conditions was reported as safe and efficient [26]. The deactivated samples were left to cool at 4 °C before further processing. All the experimental protocols were reviewed and approved as per the institutional and ethical guidelines of WIV, CAS.

2.2. Bead beating

We devised a novel mechanical extraction technique incorporating three commercially available cell-disruption RNase-free beads from NovaStar® (NZK Biotech, Wuhan, China). Beads Z (Zirconium oxide, size 0.15 mm in diameter), beads Z + C (Zirconium oxide and Chelex® 100 resin,100−200 mesh, sodium form; Bio-Rad, USA), and beads K (Ceramic, size 0.15 mm in diameter) to enhance the sensitivity of our assay when using unpurified sample input. For beads Z + C, Zirconium oxide and Chelex® 100 resin were mixed in the ratio of 1:1 (w/w). Bead bashing is generally used for mechanical disruption of bacteria and tissues difficult to lyse [27]. Owing to its high lysis capacity and not being cell-dependent, we hypothesized that it might extract virus particles encapsulated within human cells and thus lyse the viral capsid and release the RNA.

We separately transferred 250 mg of the beads to three 0.2 mL PCR tubes (Axygen Inc., CA, USA). The VTM was then gently swirled to maintain a homogeneous solution from which 50 μL of the heat deactivated clinical specimens were cautiously pipetted into tubes comprising beads, and the tubes were tightly closed. Clinical samples without beads treatment served as a control. The tubes with the samples were then vigorously vortexed on a Vortex-Genie 2 Mixer (Scientific Industries, New York, USA) at maximum speed (3200 rpm) for 5 min. After vortexing, we let the beads and any possibly generated aerosols settle down at room temperature for 1 min. We promptly obtained the supernatant for subsequent downstream processes.

To further examine the impact of our bead beating protocol on RT-LAMP detection, we conducted a systematic investigation on the treatment process. First, we independently evaluated Zirconium oxide and Chelex beads, as well as a combination of the two, on a positive swab sample with and without vortexing for 5 min. Second, a separate swab sample was mechanically lysed (with vortexing) by the beads for 5 min, followed by RNA extraction with the QIAamp Viral RNA Mini Kit (Qiagen, Hilden, Germany), as specified by the manufacturer. We then compared our mechanical lysis approach to other commonly used chemical and enzymatic lysis methods, such as lysis buffer VXL (Qiagen; active ingredient - Guanidine hydrochloride; 1:1), Igepal CA-630 (Sigma-Aldrich, Saint Louis, USA; 0.5%), proteinase K (Promega, Madison, USA; 1:1), and Recombinant RNase inhibitor (Takara Bio Inc.; 40U/μL). The sample-to-lysis buffer ratios and final concentrations used to treat the sample are represented by the ratios and concentrations in brackets, respectively. For the chemical treatments, the incubation time was 5 min. Lastly, we determined the optimal mechanical lysis time by performing our bead beating method at 1,3,5,7,10,15,20 min intervals.

2.3. RNA extraction and RT-PCR assays

We extracted total RNA from the inactivated SARS-CoV-2 cell supernatants and clinical samples using FineMag Quick Viral DNA/RNA kit-manual version. In addition, FineMag Quick Viral DNA/RNA kit-automated version was coupled with an automated machine, Purifier™ Modesty (Genfine Biotech, Beijing, China). We detected the purified RNA using an approved commercial real-time RT-PCR kit (Bioperfectus, Jiangsu, China) on a LightCycler® 480 Instrument II (Roche, Mannheim, Germany). A cycle threshold (Ct) value of <40 for SARS-CoV-2 targets and <35 for the human internal control gene was considered positive.

2.4. RT-LAMP assay and primer design

In our preliminary work [25], we designed five SARS-CoV-2 primers sets. Of which, N-A was the most sensitive primer and was used in some studies [19,20,28,29]. As a follow-up study, we designed more sensitive primer sets targeting highly conserved segments of genes encoding open reading frame 8 (*ORF8*) protein and the spike protein of SARS-CoV-2. Additionally, we designed internal control primers targeting the human ribonuclease P protein subunit p20 (RPP20) encoded by the *POP7* gene. Using the online NEB® LAMP primer design tool (https://lamp.neb.com/#!/) with default parameters, we designed three sets of primers specific for each target region. The primers were evaluated individually, and the best performing set was selected for further analysis. In silico analysis of the primers using NCBI primer-BLAST revealed 100% identity to SARS-CoV-2 and no matches for other closely related human coronaviruses. We additionally checked the frequency of mutations in the targeted segments using the CoVsurver app on the GISAID database (www.gisaid.org). The primers were synthesized by Sangon Biotech (Shanghai, China).

A 25 μL RT-LAMP reaction volume consisted of 12.5 μL of WarmStart® Colorimetric LAMP 2x Master mix with Uracil-DNA glycosylase (UDG) (New England Biolabs, Beverly, USA), 2.5 μL of 10x primer mix, 2 μL of RNA sample, 5.5 μL of sterile nuclease-free water, and 2.5 μL of Guanidine hydrochloride (40 mM final concentration). The concentration of primers used in this assay remained the same as in the previous study [25]. For colorimetric detection only, unless otherwise stated, the reaction was set at 65 °C for 30 min in a portable dry bath (MyLab, Beijing, China). A color change from pink to yellow or intermediate orange is a positive reaction.

To enable quantitative analysis, colorimetric and fluorometric assays were performed simultaneously by adding 1 μM of SYTO®-9 intercalating dye (Invitrogen, Carlsbad, USA) to the final RT-LAMP mix and incubated on CFX96 Real-Time PCR system (Bio-Rad, Hercules, CA, USA) at 65 °C. The protocol was set, unless otherwise stated, for 25 cycles (~30 min reaction time), 1 min each cycle, and the fluorescence signal was detected on the FAM channel at the end of each cycle. A sigmoid (S-shaped) curve before the threshold cut-off time was considered a positive result; otherwise, it was a negative result.

2.5. Analytical performance of RT-LAMP primers

To determine the limit of detection (LOD) of the primers, RNA dilutions were assayed in 12 replicates at each dilution. The RNA copy was determined by One-step RT-ddPCR Advanced Kit for Probes (BioRad Cat. #1864022) using primers described in our recent report [30]. The observations for each primer or primer combination were then fit in a probit curve. The LOD was defined as the least dilution at which the primers detected 95% of the replicates. The primers were multiplexed in equal ratio or according to their performance in a single-tube reaction of duplex or triplex assays.

To check the primers' specificity, we tested them against a panel of six respiratory pathogens available as laboratory stock. DNA or RNA was extracted from the following pathogens: Influenza A (H3N2, H1N1), Influenza B (Yamagata, Victoria), *Mycobacterium tuberculosis*, *Streptococcus pneumoniae*.

2.6. Optimization of primer sets by melting curve analysis and gel electrophoresis

High resolution melting curve (HRM) analysis and agarose gel electrophoresis post-amplification were used to differentiate specific from non-specific RT-LAMP products in our assay. Following temperature ramping to 95 °C for 10 s to inactivate enzymes and cooling to 60 °C for 0.05 s, melting curves were generated by temperature increment to 95 °C at a ramp rate of 0.5 °C/sec, including a plate reading step at each temperature. The BioRad's CFX 96 software manager automatically produced the melting curves at the end of the melt protocol. The products were then subjected to 2% gel electrophoresis stained by GelRed dye, run at 120 V/150 mA for 40 min. Finally, we visualized the banding patterns under UV on BioRad's ChemiDoc™ molecular imager.

2.7. Effect of sample matrix on direct approach RT-LAMP reaction system

To assess the tolerance of the LAMP mixture to VTM, we tested 1 μL−5 μL of two commercially available VTMs; VTM Y (Yocon Biology, Beijing, China) and VTM X (Xinkang Medical, Jiangsu, China). We spiked 1 mL of each VTM with 5 μL of purified extracted SARS-CoV-2 RNA. The reaction was set up as described above. We included 1 μL of the extracted RNA without VTM as a control. To further investigate the effect of crude cell lysates on the performance of the LAMP mix, we repeated the procedure, as in the case of VTM. However, an unpurified mechanically lysed positive swab sample was used as the template.

2.8. Detection of cell-cultured SARS-CoV-2 spiked in PBS and saliva samples

We also evaluated the assay's variability in detecting extracted RNA and crude lysates from simulated PBS and saliva samples. The samples were prepared, as mentioned above. In crude lysates, the samples were mechanically lysed by bead beating, and 1 μL was used as the RT-LAMP template. Primer mix S1:ORF8 (1:0.8) and human internal control primers were used in this experiment.

2.9. Calibration of template transfer tools

To facilitate the transfer of templates from sample tubes into reaction tubes at POC in the absence of pipettes, we calibrated rod-like transfer tools made of wood, plastic, metal, and glass. We selected the materials based on accessibility and ease of use. The calibration curve was constructed by measuring the absorption of GelRed® dye (Biotium, CA, USA) using ultraviolet−visible spectroscopy (UV−Vis) against its corresponding dilutions. In this case, we used a 100x dilution of the dye to act as our standard stock solution. From the stock solution, we pipetted 1 μL−5 μL and added each volume to 500 μL of sterile, nuclease-free water. The mixture was then vortexed to ensure uniformity. We run the samples in triplicate on NanoDrop™ One (Thermofisher, Massachusetts, USA) per the manufacturer's instructions. After generating the calibration curve, the same procedure was repeated, but this time with the tools to be calibrated. The tools were not only calibrated based on material but also diameter (wood = 0.25 mm, plastic = 0.20 mm, metal = 0.30 mm and glass = 0.70 mm) and height (2 mm, 4 mm, 6 mm, 8 mm and 10 mm).

2.10. Storage stability of the RT-LAMP master mix

We investigated the shelf-life of the ready-to-use RT-LAMP master mix stored at −20 °C, 4 °C, and room temperature for up to 28 days. After every two days, we tested the stability of the LAMP mix to detect a positive swab sample in four technical replicates. Note that SYTO®- 9 dye was not included in the RT-LAMP reagent-ready mix. The dye was only applied to the mixture shortly before the reaction was set.

2.11. Diagnostic evaluation of the RT-LAMP assay

A total of 143 clinical nasopharyngeal swab specimens were evaluated using our optimized direct approach RT-LAMP assay while using commercial RT-PCR kits approved by the Chinese FDA as the standard test for comparison. The experiments were performed concurrently, and the investigators were oblivious to any test outcome, not until all of the data were collected.

2.12. Statistical analysis and data processing

The normality of data was checked, and the graphs were generated by GraphPad Prism Software Windows version 8.01 (GraphPad Software, California, USA). Data are represented as mean and standard error of the mean (SEM) or mean ± standard deviation (SD), where appropriate. Unless otherwise stated, all data points are representative of three independent experiments. Two-way ANOVA with Tukey multiple comparison was used to compare the differences between groups. Statistically significant differences between groups are marked on the corresponding diagrams. The probit analysis was performed using MedCalc® software Windows version 19.3. Spearman's correlation was established between RT-PCR and RT-LAMP tests of PBS and saliva samples. Linear regression analysis between RT-PCR and ddPCR quantification of RNA was also performed. The diagnostic performance parameters for the direct approach RT-LAMP, compared to commercial RT-PCR kit on clinical swabs, were calculated using the online MedCalc's Diagnostic test evaluation calculator (https://www.medcalc.org/calc/diagnostic_test.php).

3. Results and discussion

3.1. Optimization of primer sets for sensitive and specific SARS-CoV-2 detection

Spurious amplification due to the formation of primer dimers and self-amplifying hairpins is a common problem with LAMP technology [31]. Accordingly, those interactions must be accounted for in a particular assay since they may affect the specificity and impede the speed and the sensitivity of LAMP reactions [21]. Developing a robust LAMP assay depends mainly on the performance of the primer. The high number of primers used in a single reaction may lead to non-specific amplification due to intrinsic interactions between primers, affecting detection performance. A few primer sets (N-A, N2, Orf1a-HMSe) [25,32,33] reported with high sensitivity for SARS-CoV-2 detection, and new primers designed by us (Table 1) were evaluated using high resolution melting curve (HRM) analysis and agarose gel electrophoresis after amplification.

In Fig. 1, the combination of two or three primer sets for detection resulted in either specific or non-specific amplification depending on the primer set. Gel electrophoresis showed ladder banding patterns on negative control and NTC, similar to those on dilutions 1−5 when non-specific amplification occurred (Fig. 1D). In contrast, no such ladder banding patterns were observed for negative control and NTC in case of specific amplification (Fig. 1A). The HRM analysis revealed more interesting double peaks in the case of non-specific amplification, melting temperature (*Tm*) of 84 °C at the first peak and higher *Tm* of 89 °C and 90 °C at the

Table 1
List of RT-LAMP primers designed and used in this study.

Primer	Sequence 5′-3′	Target segment
ORF8-F3	CCAAGAATGTAGTTTACAGTCAT	NC_045512.2[a]
ORF8-B3	CCTGGCAATTAATTGTAAAAGGTA	27894-28259
ORF8-FIP	TGCTGATTTTCTAGCTCCTACTCTACATCAACCATATGTAGTTGATGAC	ORF8 protein
ORF8-BIP	CCTTTAATTGAATTGTGCGTGGATCAGGAAACTGTATAATTACCGATA	
ORF8-LF	GAATAGAAGTGAATAGGACACGG	
ORF8-LB	GCTGGTTCTAAATCACCCATT	
S1-F3	GTGTTTATTACCCTGACAAAGT	NC_045512.2[a]
S1-B3	CTCTTATTATGTTAGACTTCTCAGT	21600-22100
S1-FIP	TGGAACCAAGTAACATTGGAAAAGATCAGATCCTCAGTTTTACATTC	Spike protein
S1-BIP	GCTATACATGTCTCTGGGACCAATGGAAGCAAAATAAACACCATCA	
S1-LF	AGGTAAGAACAAGTCCTGAGTT	
S1-LB	GGTACTAAGAGGTTTGATAACCCT	
RPP20-F3	GGTGGCTGCCAATACCTC	GeneBank U94316.1[a]
RPP20-B3	ACTCAGCATGCGAAGAGC	Ribonuclease P Subunit P20
RPP20-FIP	GTTGCGGATCCGAGTCAGTGGCCGTGGAGCTTGTTGATGA	
RPP20-BIP	AACTCAGCCATCCACATCCGAGTCACGGAGGGGATAAGTGG	
RPP20-LF	TCCCGTGTGTCGGTCT	
RPP20-LB	TCTTCAGGGTCACACCCA	

Additional primer sets (N-A, N2, Orf1a-HMSe) were adapted from other studies [25,32,33].
[a] GeneBank accession numbers for the target segments.

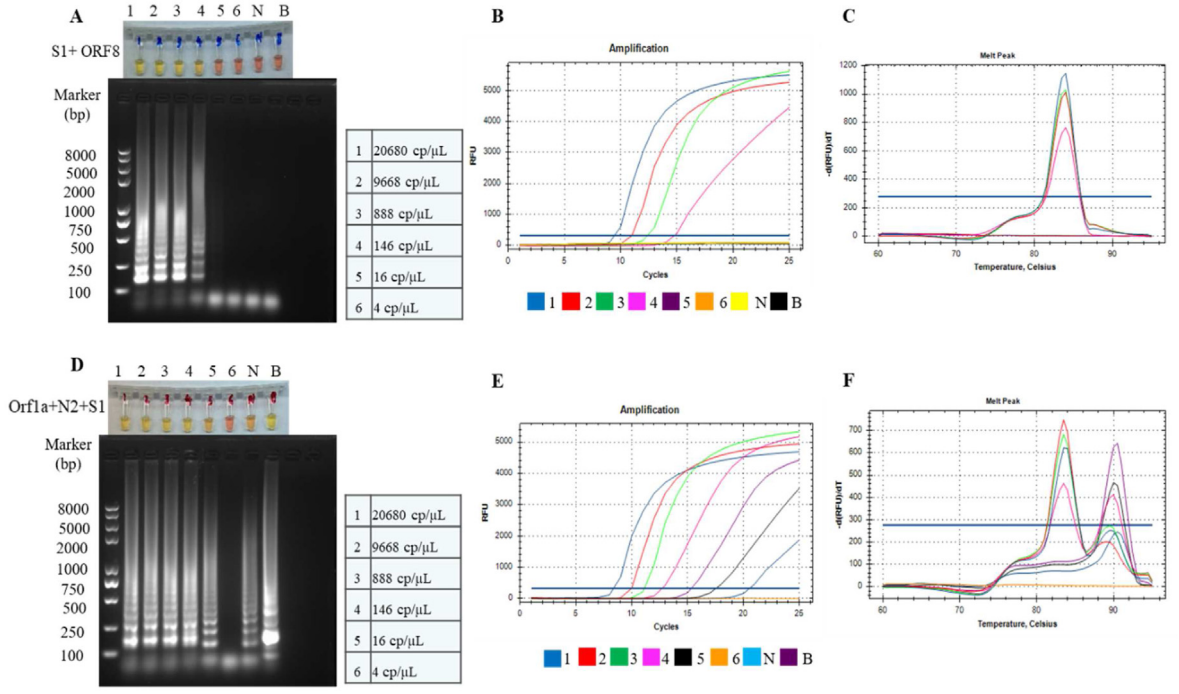

Fig. 1. Discrimination between specific and non-specific RT-LAMP amplification of different primer sets. (A) 2% Gel electrophoresis and colorimetric, (B) fluorometric, and (C) melting curve profiles for specific amplification by primers S1 + ORF8 post-amplification.'1–6' are SARS-CoV-2 RNA dilutions. 'N'-negative control, 'B'-no template control. (D) 2% Gel electrophoresis and colorimetric, (E) fluorometric, and (F) melting curve profiles post-amplification for non-specific amplification using primers Orf1a-HMSe + N2 + S1. Primer Orf1a-HMSe and N2 adapted from other studies [32,33].

second peaks (Fig. 1F), and only single peak, *Tm* of 84 °C, in the case of specific amplification (Fig. 1C). The NTC showed no peaks in specific amplification but a single peak with a higher *Tm* of 91 °C in non-specific amplification. Intriguingly, as the template concentration decreased, the greater the probability of double peaks or single peaks with higher *Tm*. Based on the HRM analysis, the primer sets S1 and ORF8 designed newly by us, N-A reported previously by us, and RPP20 to detect the human internal control were found quite specific for the detection (Appendix A Figs. S2 and S3). Additional peaks with higher *Tm* seen in non-specific reactions may be due to stable secondary DNA structures requiring higher *Tm* dissociation. The double peaks in the presence of the template may imply the simultaneous occurrence of specific and non-specific amplification. Conversely, the melting peaks in SYBR green real-time PCR due to non-specific amplification have lower *Tm* [34]. We speculate that the difference is because LAMP generates a large amount of DNA amplicons compared to PCR. Like in PCR, the melting profile of LAMP products is primarily dependent on GC content, sequence and length of the amplicons [35]. Gel electrophoresis can confirm the formation of a specific product in PCR with a single band of a given size. However, since LAMP produces heterogeneous products of stems and loop, the correct banding pattern of a specific amplification might be challenging to discern from that of non-specific amplification. Therefore, HRM analysis is a

simpler and more reliable method to detect false-positive amplification in LAMP reactions than gel electrophoresis, which is routinely used to develop LAMP assays.

Another feature of LAMP is that non-specific amplification will eventually occur if the reaction time is prolonged. In theory, the accumulation of background signals in non-template reactions occurs as the reaction progresses. The melting curve analysis was used to determine when non-specific products were starting to form for the primer set S1:ORF8 (1:0.8). As shown in Appendix A Figs. S4 and S5, non-specific amplification was observed at the reaction time of 40 min. The cut-off for primer set S1:ORF8 (1:0.8) in the following experiments was set at 30 min (reaction time) for colorimetric assay or 25 cycles (threshold time) when monitoring real-time fluorescence of the LAMP on the PCR instrument, unless stated otherwise.

3.2. Analytical performance of RT-LAMP primers used in this study

To evaluate the sensitivity of the primers, five-fold serial dilutions of SARS-CoV-2 RNA from cell culture were used. The dilutions were quantified by RT-ddPCR (Appendix A Fig. S1). S1 primer was found the most sensitive compared to ORF8 and N-A (Fig. 2A and B). The human internal control primer, RPP20, also performed relatively well on human gene dilutions. Of note, we used an inactivated whole virus rather than synthetic RNA transcripts as the standard control; hence a higher limit of detection (LOD) compared to other studies reporting similar performance to RT-PCR with lower LOD [36]. Zhou et al. [37] recently reported that a whole virus quantified by RT-ddPCR would provide an ideal reference standard for quality control assessment from nucleic acid extraction to detection. Absolute quantification by RT-ddPCR enables a more accurate determination of amplifiable RNA copies compared to estimation by molecular weight.

We further tested whether primer multiplexing could increase the sensitivity of our assay. We observed that multiplexing the primers in ratios proportional to their performance resulted in more sensitive reactions than when the primers were mixed in equal ratio, either as duplex or triplex assays (Fig. 2C and D). Primer multiplexing using Guanidine hydrochloride can improve the speed and sensitivity of colorimetric LAMP [32]. Moreover, multiplexing may help keep up with potential primer mismatches due to gene mutation, particularly with the emergence of new COVID-19 variants. However, multiplexing of primers in bulk reactions should be assessed according to a given situation. To define the LOD, we tested each primer or different primer mix in twelve technical replicates for each dilution (Appendix A Table S1). We analyzed the results with a probit curve. The lowest dilution in which 95% of the replicates were detected was LOD. Primer mix S1:ORF8 (1:0.8) was the most sensitive set, followed by S1 primer (Fig. 2G and H). None of the respiratory pathogens tested cross-reacted with the primers (Fig. 2E and F).

3.3. Effect of sample matrix on direct RT-LAMP reaction

Many reports have been published on RT-LAMP detection of SARS-CoV-2 after extracting RNA [38–40]. This step not only adds time to detection workflows but also makes operation outside centralized laboratories difficult. Since LAMP is more tolerant than RT-PCR to inhibitors in the samples, we next tested if RT-LAMP could detect SARS-CoV-2 directly from swab samples (direct RT-LAMP approach) collected in two commercial viral transport media (VTM; Y and X). In fluorometric detection, the LAMP mix using the primer set N-A showed more resistance to a larger volume of VTM Y (Fig. 3B) than VTM X (Fig. 3D). The inversion of fluorescent

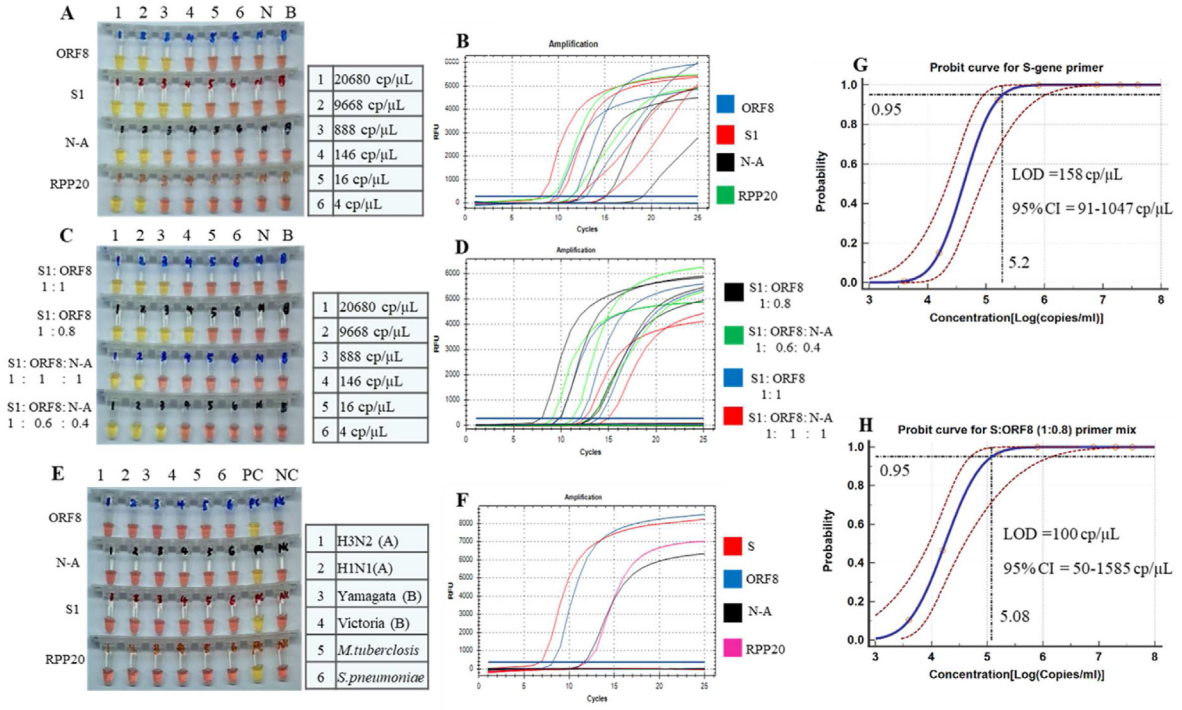

Fig. 2. Analytical performance of primers for SARS-CoV-2 and human internal control detection. (A, B) Sensitivity of ORF8, S1, and N-A primers tested in 5-fold serial dilutions of SARS-CoV-2 RNA (1–6). RPP20 primers in dilutions of human gene (1–4), 'S'- SARS-CoV-2 RNA, 'N'- negative control, 'B'- no template control, cp/µL - RNA copies/µL. (C, D) Primer multiplexing in different ratios. (E, F) Specificity of primers against other respiratory pathogens. 'PC'-positive control, 'NC'-negative control. (G, H) Probit curve reflects observations from twelve replicates at each dilution. LOD is the least dilution at which 95% of the replicates are detected. Red dotted curves are confidence intervals. (For interpretation of the references to color in this figure legend, the reader is referred to the Web version of this article.)

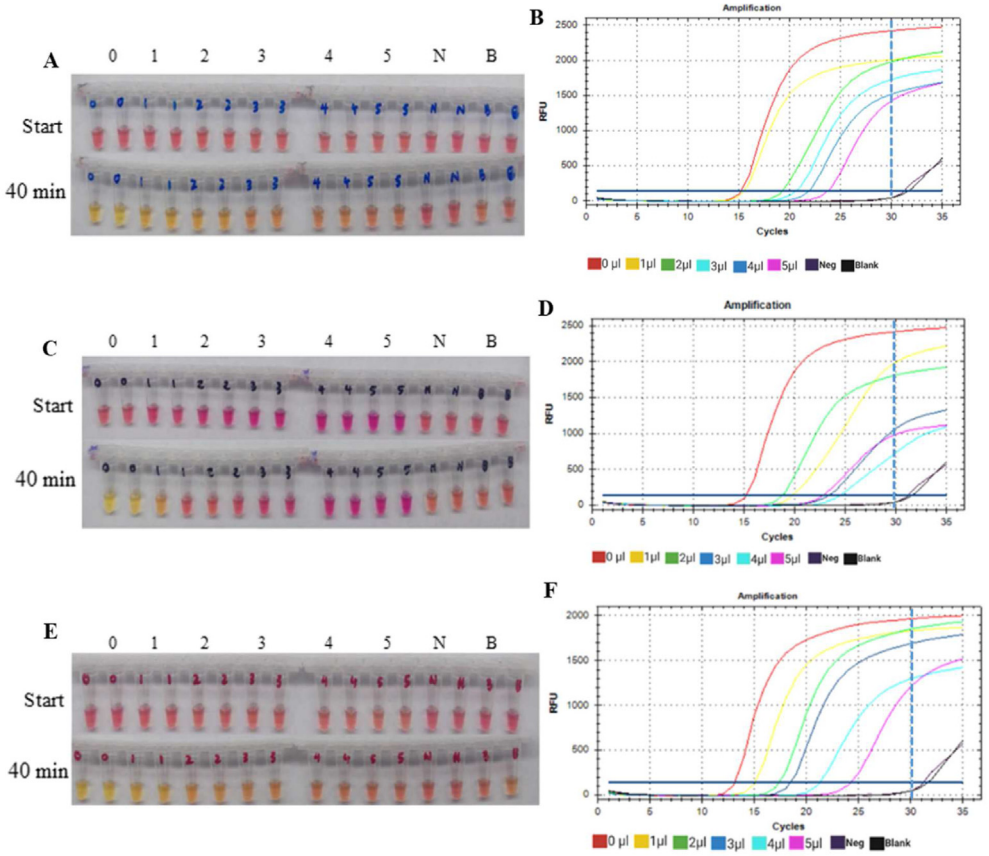

Fig. 3. Effect of sample matrix on the direct RT-LAMP assay based on primer N-A. Tolerance of the RT-LAMP reagents to 1 μL–5 μL of VTM Y (A, B) and VTM X (C, D). Extracted SARS-CoV-2 RNA was used as the template. '0' denotes no VTM used, 'N'-negative control, 'B'-no template control. (E, F) 1 μL–5 μL mechanically lysed clinical sample tested to evaluate the tolerance of the system to crude human cell lysates. Here, '0' denotes using purified RNA extracted from the mechanically lysed clinical sample in VTM Y as the template. The dashed line indicates the 30 min (35 min reaction time) threshold time cut-off for this experiment.

curves in VTM X was observed in three independent experiments. Generally, with an increase in the volume of VTM, there was a corresponding decrease in fluorescence intensity. The best amplification was recorded at adding 1 μL of VTM Y or 2 μL of VTM X. As for colorimetric detection, an increase in the VTM increased masking of color change. A positive color change was not observable by a naked eye under all volumes of VTM X (Fig. 3C) and above 3 μL of VTM Y (Fig. 3A). The above observations could be due to the corresponding rise in buffered salt solutions, antimicrobials, and amino acids used in VTMs, which could affect *Bst* enzyme activity. The typical appearance of VTM (pink/red color) could be causing masking of color change. These results underline the importance of selecting a suitable VTM compatible with a given detection method. The concept of colorimetric detection demonstrated in this study is based on the color change of pH-sensitive dyes from pink (negative) to yellow (positive) due to nucleotide incorporation during amplification [41]. On the other hand, fluorometric detection is enabled by adding intercalating dye SYTO®-9, which has a non-inhibitory effect on real-time detection with LAMP even at higher concentrations of 2–10 μM [42].

Next, we explored the effects of crude cell lysates on the RT-LAMP system. A robust color change was observed at 1 μL, and weak color changes resulted in volumes from 2 μL to 5 μL in VTM Y (Fig. 3E) and for fluorometric detection (Fig. 3F). This observation is attributed to complex biological matrices in swabs like lysed human cells, mucosal secretions, and endogenous RNases. Based on the above results, 1 μL of sample in VTM Y was found suitable for the direct RT-LAMP assay.

3.4. Mechanical lysis of clinical samples by bead beating

Since direct use of swabs in VTM is possible for RT-LAMP detection, it is apparent that efficient lysis of viral particles sequestered within human cells and release of viral RNA would be beneficial for sensitive detection. Results on bead beating showed that beads Z + C were the most efficient in lysis than beads Z, beads K, and the control (Fig. 4). This phenomenon was consistent in all the five clinical samples tested (Appendix A Fig. S6). Notably, for sample 5, no amplification was observed when the sample was treated with beads Z, K, and the control (Fig. 4A). Compared to sample 2, there were significant differences in RT-LAMP Tt between beads Z + C, control and other beads (Fig. 4B and C). According to RT-PCR, the cycle threshold (Ct) values for samples 1 to 5 were: 29.11, 32.46, 31.27, 34.06, and 34.95, respectively. The mechanical ability of beads to lyse cells is attributed to large shear forces between beads and strong vortical flow fields [43]. The cell ruptures when the kinetic energy of colliding beads exceeds the elastic energy contained within the cell [44]. Mechanical lysis is more effective than chemical, thermal, or electrical lysis because no inhibitors or reagents are introduced, and nucleic acids are not destroyed by high temperatures [45]. Because mechanical stress, like thermal stress, can cause protein aggregation and precipitation due to protein conformational changes [46], it is possible that mechanical lysis could lyse viral capsid and release viral RNA. Recently, it was reported that the addition of microparticles such as beads might aid in the generation of high mechanical stress by creating vortex flow [47].

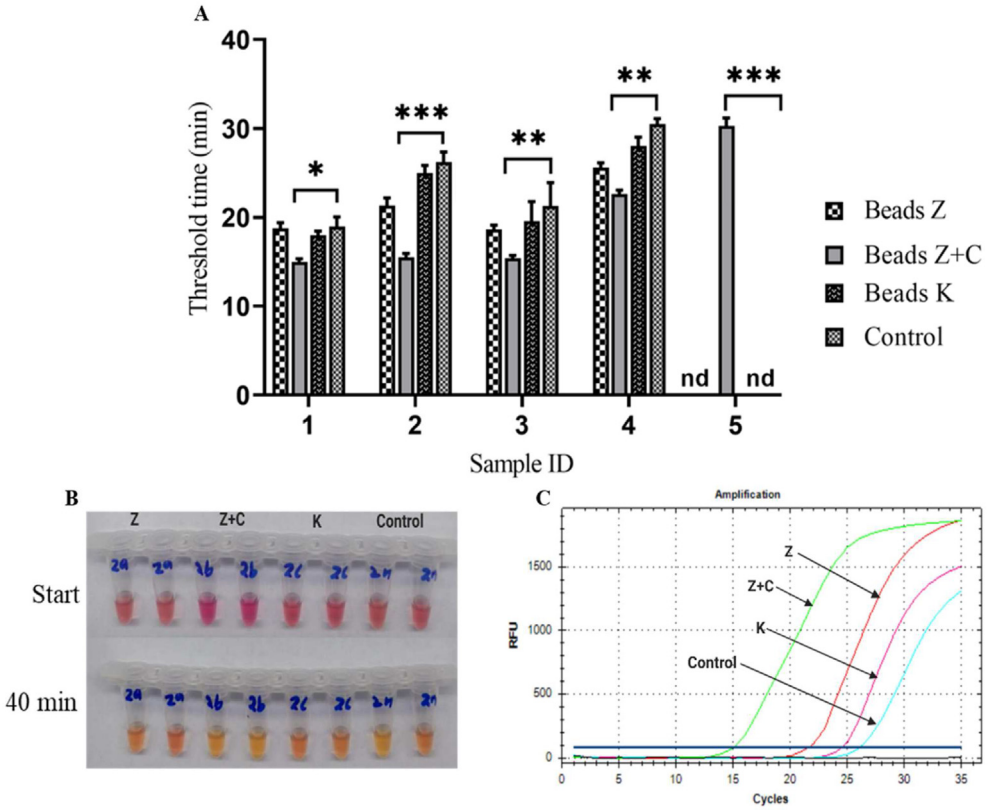

Fig. 4. Comparison of mechanical lysis effectiveness for three different beads (Z, Z + C, K) and control (No beads) on selected five positive clinical swab samples. (A) The Tt represents three independent experiments (duplicate technical replicates) and denotes mean and SD. Two-way ANOVA with Tukey multiple comparison was used to compare the differences between groups (Differences between groups with beads Z + C treatment and control are shown). Statistically significant differences are marked *, **, ***, indicating $p < 0.05$, $p < 0.01$, $p < 0.001$, respectively. 'nd' = not detected. '2n' = no bead treatment for sample 2. (B) Colorimetric and (C) Fluorometric detection for sample 2. Primer N-A was used in this experiment. The corresponding colorimetric and fluorometric results are shown in Appendix A, Fig. S6.

The addition of samples lysed by Beads Z + C did not interfere with the original pink color of the RT-LAMP master mix, suggesting minimal disruption of pH-sensitive dyes. A plausible explanation is that Chelex is weakly acidic and a chelating agent with a high affinity for divalent metal ions and can bind to Mg^{2+}, a cofactor for enzyme activation. This property could aid in the deactivation of RNases [48]. On the contrary, the master mix color slightly changed when samples were lysed with other beads (Fig. 4B). Remarkably, using Beads Z + C improved the sensitivity and the reproducibility of the direct RT-LAMP assay, and thus the combination of beads was used in subsequent experiments. Other studies used RNase inhibitors, lysis buffers or proteinase K for sample lysis; however effective, they can act as potential LAMP inhibitors unless they are purified or deactivated [33,36,49]. Recently, magnetic bead-based RNA extraction protocol and hybridization capture methods were described [50,51]. Although these methods yield purified RNA, they involve multiple steps of washing and suspending beads, increasing the sample processing time and the risk of cross-contamination among samples. The bead beating method described here is a streamlined process that does not have centrifugation and elution steps, which could lead to sample loss. Since the requirement of a vortex may weaken the portability of our system, we recommend a disposable, battery-powered, miniaturized Omnilyse device (Claremont Biosolutions, USA). The device is based on a bead beating technique; the same results can be obtained by simply incorporating the beads identified in this study.

3.5. The impact of mechanical lysis with Zirconium oxide and Chelex on RT-LAMP

To unequivocally demonstrate the impact of the bead beating approach, we chose the combination of Zirconium oxide (ZrO_2) and Chelex beads that performed best in the prior experiment. In comparison to other treatments, combining ZrO_2 and Chelex with vortexing improved RT-LAMP detection for SARS-CoV-2 the greatest, as shown in Fig. 5A. Even though chemically inert ZrO_2 can induce cell lysis and subsequent RNA release from virus particles via mechanical force, the RNA remains vulnerable to degradation by RNases and other contaminants in the sample. Guan et al. [52] recently reported that Chelex resin preserves SARS-CoV-2 RNA in common buffers allowing direct RT-PCR detection; therefore, we believe the inclusion of Chelex in the VTM sample is crucial in protecting released RNA templates from degradation by endogenous RNases. In contrast to the no-vortexing condition, we speculate vortexing in the presence of ZrO_2 generates mechanical force and thoroughly mixes the Chelex with the contaminants in the sample.

For all the treatment groups, the subsequently extracted samples had shorter RT-LAMP threshold times (Tt) than the mechanically lysed samples (Fig. 5B). We observed slight variations in the Tt of the extracted samples across all treatments. The observation is logical because extraction eliminates all other potential influences on the detection reaction other than RNA concentration. However,

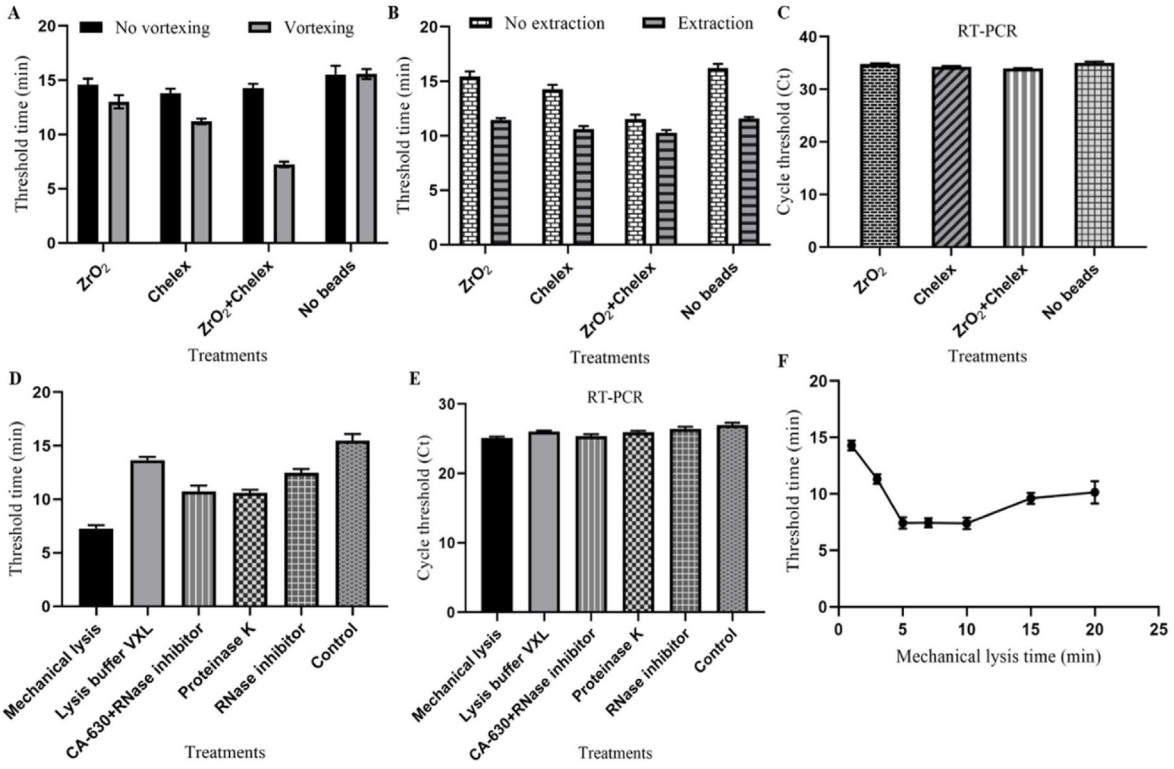

Fig. 5. The impact of mechanical lysis with Zirconium oxide and Chelex on RT-LAMP detection. (A) Effect of vortexing and no vortexing on mechanical lysis of a positive swab sample. (B) Effect of no extraction and subsequent RNA extraction of a mechanically lysed swab sample. (C) RT-PCR detection of extracted RNA from the mechanically lysed sample (D) Mechanical lysis versus other common lysis modalities. (E) RT-PCR detection of extracted RNA from mechanically lysed sample compared with other lysis methods (F) The effect of mechanical lysis time on the release of SARS-CoV-2 RNA. Primer S1:ORF8 (1:0.8) was used in this experiment. Data represent the means ± SD of three technical replicates. The corresponding colorimetric and fluorometric results are shown in Appendix A, Figs. S7 and S8.

depending on the method used for extraction, some studies have reported RNA loss as a result of RNA extraction [50,52]. The Tt difference between extracted and non-extracted samples was lowest in the ZrO_2 and Chelex group when compared to other treatments (Fig. 5B). This indicated that ZrO_2 and Chelex beads could help in the release of more viral RNA and the absorption of potential interferences in the sample, even without the RNA extraction step. To ensure that the beads are producing more target RNA rather than more LAMP signals for unrelated reasons, we further detected the extracted samples using RT-PCR. Indeed, we made a similar observation as in RT-LAMP (Fig. 5C), confirming that the shorter Tt could be due to more target RNA produced. Because neither ZrO_2 nor Chelex beads dissolve in VTM, they are allowed to settle after vortexing, and the supernatant is used as the template directly. As a result, no carry-over beads are permitted in RT-LAMP reactions, and possible inhibition is avoided. Our mechanical lysis method outperformed conventional chemical and enzymatic lysis modalities (Fig. 5D). RT-PCR could detect the extracted samples from the various lysis methods, verifying the production of target RNA in all of the lysis methods (Fig. 5E). Although proteinase K can successfully lyse samples, it must be heat-deactivated at 95 °C for 5 min to avoid inhibiting RT-LAMP reactions, which may further destroy RNA [53]. On the other hand, RNase inhibitor can protect liberated RNA from degradation by endogenous RNases but is unable to liberate RNA within viral envelopes or human cells. The tested concentrations of lysis buffer VXL and non-ionic detergent Igepal CA-630 appeared to be compatible with RT-LAMP; however, more studies are needed to determine their impact on viral particle lysis. To ensure complete sample lysis and effective RNA release, we determined the appropriate mechanical lysis time. The optimal lysis time was found to be 5 min (Fig. 5F).

We finally validated our mechanical bead lysis method against a no-bead control with 32 clinical swab samples. As detected by RT-LAMP, the amount of amplifiable RNA increased substantially across all samples (Appendix A Table S8). However, we observed that the magnitude of the detectable RNA increase varied amongst samples, even those with the same viral load as measured by RT-PCR. The phenomena could be explained by the fact that different samples may contain inhibitors or components that others do not, for example, tobacco substances, nasal sprays, and mouth wash chemicals. Regardless of the variation, our mechanical lysis method ensures an accurate and reliable qualitative SARS-CoV-2 detection, which is critical in a point-of-care setting.

3.6. SARS-CoV-2 detection in simulated phosphate-buffered saline (PBS) and saliva samples

Saliva is a more reliable diagnostic specimen for SARS-CoV-2 than nasopharyngeal swabs [54]. Also, PBS is a potential alternative to VTM [55]. Interestingly, the RT-LAMP assay was slightly more sensitive to the crude lysate (Fig. 6E and F) than extracted RNA (Fig. 6A and B) for PBS and saliva. This may be due to sample loss during RNA extraction as a result of the repetitive steps of beads washing, suspension, and sample elution. However, RT- PCR Ct was strongly correlated to RT-LAMP Tt for the extracted RNA (Fig. 6D) than for the crude lysate (Fig. 6H). Overall, these results

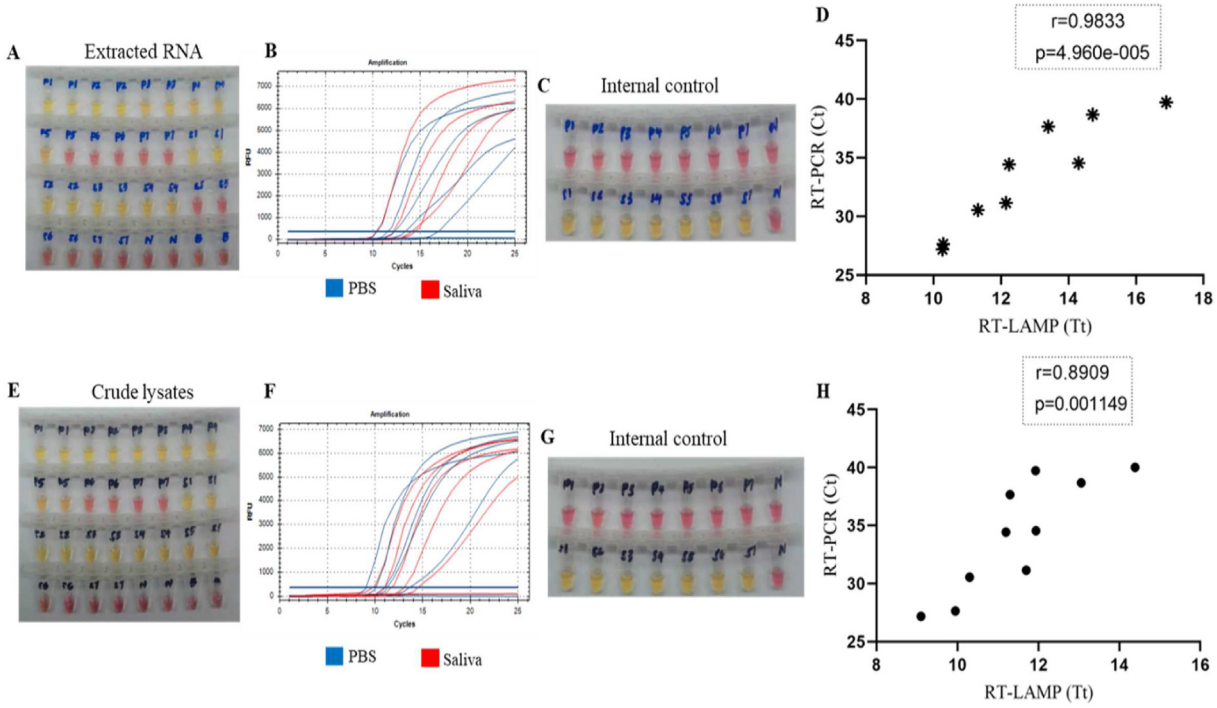

Fig. 6. Detection of cell-cultured SARS-CoV-2 spiked in 1x phosphate-buffered saline (PBS) and saliva samples in 10-fold dilution series. (PBS, P1-P7) (Saliva, S1-S7). (A, B, C, D) Detection of extracted RNA from PBS and saliva samples. (E, F, G, H) Detection of crude lysates from mechanically lysed PBS and Saliva samples. (A and E, B and F) Colorimetric and fluorometric readouts, respectively. (C, G) Detection of human internal control gene using RPP20 primers. (D, H) Spearman's correlation of RT-PCR with RT-LAMP for PBS and Saliva samples. Primer S1:ORF8 (1:0.8) was used in this experiment.

demonstrate the utility of our bead beating protocol and support the hypothesis that mechanical lysis can improve RT-LAMP detection sensitivity for SARS-CoV-2 without necessarily purifying the template. It is worth mentioning that the commercial RNA extraction kit used in this study is based on magnetic beads system. As expected, the internal control gene was detected in the saliva and not in the PBS samples (Fig. 6C and G). No masking of color change by PBS or saliva was observed, as seen in the colorimetric LAMP when swabs in VTM were used.

3.7. Calibration of template transfer tools

It is not always possible to have all the equipment and adequate skilled persons to operate in resource-limited decentralized settings. In order to provide a simple way of transferring a small volume of liquid for RT-LAMP reaction, we thought rod-like tools could be used (Fig. 7C). To ensure the accuracy and precision of transfer tools at our disposal that could be used for the template transfer, we generated a standard curve of GelRed® dye using a calibrated pipette (Fig. 7A). Using the curve, volumes transferred using rods made of different materials with different sizes were measured,

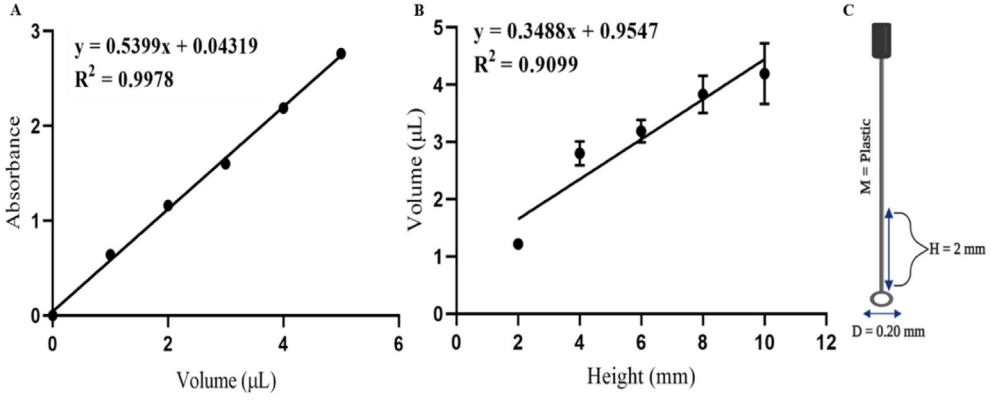

Fig. 7. Calibration of template transfer tool. (A) Standard curve for UV−Vis absorbance of GelRed dye against the volumes transferred using a calibrated pipette. The absorbance was measured of 1 µL−5 µL of the dye, each diluted in 500 µL of sterile clean water. The measurements were performed in duplicate at wavelength of 450 nm. Data represented here is mean absorbance against volume. (B) A linear relationship between volumes transferred with the calibrated template transfer tool based on the standard curve against insertion height of transfer tool (Appendix A Table S7). (C) Schematic representation of the calibrated template transfer tool. M, Material; H, Height; D, Diameter. The plastic tool at the insertion height of 2 mm was used for the template transfer.

Table 2
Interpolated data of the unknown (volume) from the calibration curve.

Material	Diameter (mm)	Absorbance (Mean ± SD)	Volume (μL) (Mean ± SD)
Plastic	0.20	0.58 ± 0.02	1.01 ± 0.03
Wood	0.25	1.87 ± 0.04	3.39 ± 0.08
Metal	0.30	2.51 ± 0.01	4.58 ± 0.02
Glass	0.70	OVERFLOW[a]	N/A

Abbreviations: mm, millimeter; μL, microliter; SD, standard deviation; N/A, not applicable.
[a] Absorbance out of range that can be detected by NanoDrop™ One instrument.

and we obtained measurements summarised in Table 2. It can be seen that volumes ranging from 1 μL to 5 μL could be transferred by suitable rods with relatively good reproducibility, which might facilitate adding a template for LAMP reaction on sites without pipettes. We further calibrated wood (diameter = 0.25 mm) and plastic (diameter = 0.20 mm) tools based on height as shown in Appendix A Tables S3, S4, S5, S6, and S7. We noticed that the height parameter greatly influenced the degree of variation in template volume transferred. Thus caution should be exercised when tools are immersed vertically in reaction tubes to avoid sampling errors. The calibrated manual transfer tool could transfer 1 μL volumes with better accuracy and consistency than the volumes above 2 μL (Fig. 7B). In our case, the plastic tool immersed in reaction tubes at the height of 2 mm proved to be the most convenient and was therefore used in place of pipettes to transfer 1 μL of the template.

3.8. Shelf-life of the RT-LAMP master mix

The master mix was found most stable when stored at −20 °C and least stable at room temperature (Appendix A Table S2). We also found that storing the master mix inclusive of SYTO®- 9 dye at −20 °C could reduce its stability after three weeks of storage (data not shown). Hence, the SYTO®- 9 dye was not included in the master mix during storage. Additionally, extended freeze-thaw cycles of the stored master mix should be avoided, as this was observed to degrade the stability of the master mix.

3.9. Diagnostic evaluation of the direct RT-LAMP assay

We proposed a direct RT-LAMP assay without RNA extraction for optimal point-of-care testing of COVID-19, as shown in Fig. 8. The performance of the system was compared to commercial RT-PCR kits detecting RNA extracted from clinical nasopharyngeal swabs. Validation was conducted in two screening rounds. In the first round, we used the primer set N-A, which performed best in our previous study [25]. The direct approach RT-LAMP using primer N-A had a 93% overall agreement with RT-PCR (Table 3). Two false-positive cases were observed, and eight samples with low viral loads (Ct > 35) were not detected either by the colorimetric or the fluorometric assays. Interestingly, we noted that the fluorometric detection (up to PCR Ct of ~34.94) was more sensitive than colorimetric detection (up to PCR Ct of ~32.93) (Appendix B Table S1). The inconsistency may be because pH-sensitive dyes are more vulnerable to inhibitors in the sample than SYTO®-9 dye. This occurrence could make colorimetric RT-LAMP results subjective. Our work using the primer N-A alone has improved the sensitivity to 90.48% compared to 86% in a study using the same primer set [19]. The enhanced sensitivity of our study is that we included mechanical lysis after heat deactivation. The mechanical step could ensure more efficient lysis of samples. To our knowledge, this is the first SARS-CoV-2 detection study to use mechanical lysis for sample preparation.

In the second round, we used primer set S1:ORF8 (1:0.8) and observed improved performance of 99.3% accuracy (Table 3). Sample 76 (high Ct of 36) was not detected by either our assay or

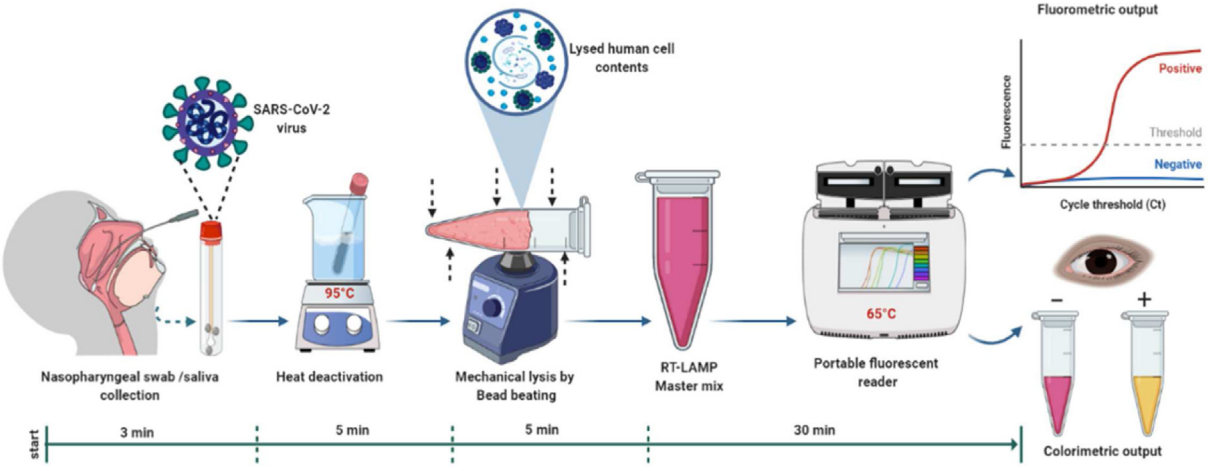

Fig. 8. Schematic illustration of the direct approach RT-LAMP workflow. After sample collection in VTM, the sample is heat deactivated at 95 °C for 5 min, then mechanically lysed by bead beating method for 5 min. Following lysis, 1 μL of the sample is added to 24 μL of ready-made RT-LAMP master mix using a pipette or the calibrated transfer tool. The reaction is then set up on a portable, battery-operated fluorescent reader (Genie® III; OptiGene Limited, UK). The results can be viewed in a fluorometric and colorimetric output after 30 min of incubation. At the point-of-care, the standard vortex can be replaced by a disposable, battery-powered, miniaturized Omnilyse device (Claremont Biosolutions, USA). All steps should be taken with complete personal protective equipment and all waste disposed off appropriately. The figure was created with BioRender.com and Mindthegraph.com.

Table 3
Diagnostic performance of direct approach RT-LAMP compared to RT-PCR.

Test	RT-PCR		Total	Sensitivity (%)	Specificity (%)	PLR	NLR	Accuracy (%)
	+	-		(95% CI)	(95% CI)	(95% CI)	(95% CI)	(95% CI)
RT-LAMP + (N-A)[a]	76	2	78	90.48 (82.09–95.80)	96.61 (88.29–99.59)	26.69 (6.82–104.41)	0.10 (0.05–0.19)	93.01 (87.52–96.60)
RT-LAMP − (N-A)[a]	8	57	65					
RT-LAMP + (S1 + ORF8)[b]	83	0	83	98.81 (93.54–99.97)	100 (93.94–100)	N/A	0.01 (0.00–0.08)	99.30 (96.17–99.98)
RT-LAMP − (S1+ ORF8)[b]	1	59	60					
Total	84	59	143[c]					

Abbreviations: CI; Confidence Interval; PLR, Positive Likelihood Ratio; NLR, Negative Likelihood Ratio; N/A, Not Applicable.
The diagnostic parameters were calculated using the online MedCalc' Diagnostic test evaluation calculator (https://www.medcalc.org/calc/diagnostic_test.php).
[a] Primer N-A used in the initial screening.
[b] primer mix S1+ORF8 (1:0.8) used in the second screening.
[c] Total number of clinical samples tested. Comparison between RT-PCR and RT-LAMP performance on the individual clinical samples is shown in Table S1 (Primer N-A) and S2 (Primer S1+ORF8) (see Appendix B).

RT-PCR during the second test, which may be judged negative based on the instruction of the kit (Appendix B Table S2). The colorimetric readouts were consistent with the fluorometric results in all the samples tested. To ascertain the performance of the RT-LAMP compared to RT-PCR, we additionally benchmarked it against two other commercially approved RT-PCR kits (Daan Gene and Sansure Biotech, China). Our test results were identical to these two kits (data not shown). The correlation between Ct values and viral infectivity showed that the RT-PCR cut-off value for SARS-CoV-2 infectivity was 34 cycles [56]. Although, cell culture infectivity is just a surrogate marker for SARS-CoV-2 infection since the virus could infect its natural host more efficiently than cell culture. The fact that our system could detect samples with low viral loads above the RT-PCR cycle threshold that is considered infectious or transmissible makes it appealing for clinical application. As such, we have demonstrated the diagnostic utility of our RT-LAMP system, which may be used to trace symptomatic and asymptomatic individuals and control the spread of SARS-CoV-2. To facilitate rapid adoption of our protocol, we prepared a standard operating procedure (SOP), provided in the supplementary material (appendix A). Based on this SOP, we estimate the cost per test to be ~3 US dollars.

However, we believe further optimizations involving sample volume, lysis time, and beads size would improve the performance of the mechanical lysis method. Our RT-LAMP system would require an unbroken cold chain to maintain the quality of the master mix. Consequently, our current work aims to stabilize the RT-LAMP master mix to facilitate shipment and storage at ambient temperatures.

4. Conclusions

In conclusion, a direct approach RT-LAMP system was successfully developed, which could detect SARS-CoV-2 within 40 min, not only from patients' swabs samples but also saliva samples. To our knowledge, this is the first SARS-CoV-2 detection study that has used mechanical lysis to improve sample preparation and calibrated a simple template transfer tool to replace pipettes. The system shows an accuracy as high as 99.3% in detecting SARS-CoV-2 from the swab samples compared to commercial RT-PCR kits approved by the Chinese FDA. Compared with many other RT-LAMP tests for SARS-CoV-2 reported so far, the current system is either easier for point-of-care testing, cheaper or faster (Appendix A Table S9). By leveraging its simplified sample preparation and optimized workflow, the system is applicable for rapidly detecting SARS-CoV-2 outside centralized laboratories.

Funding

This work was financially supported by the Wuhan Institute of Virology, Chinese Academy of Sciences Grant number: 2021005.

CRediT authorship contribution statement

Nelson Odiwuor: Conceptualization, Methodology, Writing – original draft, Investigation, Formal analysis, Validation, Writing – review & editing. **Jin Xiong:** Investigation, Formal analysis, Validation, Writing – review & editing. **Faith Ogolla:** Investigation, Formal analysis, Validation, Writing – review & editing. **Wei Hong:** Investigation, Formal analysis, Validation, Writing – review & editing. **Xiaohong Li:** Investigation, Formal analysis, Validation, Writing – review & editing. **Fazal Mehmood Khan:** Formal analysis, Validation, Visualization. **Nuo Wang:** Formal analysis, Validation, Visualization. **Junping Yu:** Formal analysis, Validation, Visualization. **Hongping Wei:** Conceptualization, Methodology, Writing – original draft, Project administration, Funding acquisition, Supervision, Resources, Writing – review & editing.

Declaration of competing interest

The authors declare that they have no known competing financial interests or personal relationships that could have appeared to influence the work reported in this paper.

Acknowledgments

We thank Dr. Nathan Tanner and Dr. Yinhua Zhang of New England Biolabs, USA, for constructive feedback on optimizing the RT-LAMP assay. We thank the Wuhan National Biosafety Lab for allowing us to use the P2 and P3 labs. We also acknowledge the support of the UCAS scholarship to International Students, the ANSO scholarship for young talents, and the Sino-Africa Joint Research Centre.

Appendix A. Supplementary data

Supplementary data to this article can be found online at https://doi.org/10.1016/j.aca.2022.339590.

References

[1] D.K.W. Chu, Y. Pan, S.M.S. Cheng, K.P.Y. Hui, P. Krishnan, Y. Liu, D.Y.M. Ng, C.K.C. Wan, P. Yang, Q. Wang, M. Peiris, L.L.M. Poon, Molecular diagnosis of a novel coronavirus (2019-nCoV) causing an outbreak of pneumonia, Clin. Chem. 66 (2020) 549–555.

[2] F. Fenollar, A. Bouam, M. Ballouche, L. Fuster, E. Prudent, P. Colson, H. Tissot-Dupont, M. Million, M. Drancourt, D. Raoult, P.E. Fournier, Evaluation of the panbio COVID-19 rapid antigen detection test device for the screening of patients with COVID-19, J. Clin. Microbiol. 59 (2021).

[3] R. Antiochia, Developments in biosensors for CoV detection and future trends, Biosens. Bioelectron. 173 (2021) 112777.

[4] G. Qiu, Z. Gai, Y. Tao, J. Schmitt, G.A. Kullak-Ublick, J. Wang, Dual-functional plasmonic photothermal biosensors for highly accurate severe acute respiratory syndrome coronavirus 2 detection, ACS Nano 14 (2020) 5268–5277.

[5] D. Liu, C. Ju, C. Han, R. Shi, X. Chen, D. Duan, J. Yan, X. Yan, Nanozyme chemiluminescence paper test for rapid and sensitive detection of SARS-CoV-2 antigen, Biosens. Bioelectron. 173 (2021).

[6] G. Seo, G. Lee, M.J. Kim, S.H. Baek, M. Choi, K.B. Ku, C.S. Lee, S. Jun, D. Park, H.G. Kim, S.J. Kim, J.O. Lee, B.T. Kim, E.C. Park, S. Il Kim, Rapid detection of COVID-19 causative virus (SARS-CoV-2) in human nasopharyngeal swab specimens using field-effect transistor-based biosensor, ACS Nano 14 (2020) 5135–5142.

[7] X. Zhu, X. Wang, L. Han, T. Chen, L. Wang, H. Li, S. Li, L. He, X. Fu, S. Chen, M. Xing, H. Chen, Y. Wang, Multiplex reverse transcription loop-mediated isothermal amplification combined with nanoparticle-based lateral flow biosensor for the diagnosis of COVID-19, Biosens. Bioelectron. 166 (2020).

[8] J.P. Broughton, X. Deng, G. Yu, C.L. Fasching, V. Servellita, J. Singh, X. Miao, J.A. Streithorst, A. Granados, A. Sotomayor-Gonzalez, K. Zorn, A. Gopez, E. Hsu, W. Gu, S. Miller, C.Y. Pan, H. Guevara, D.A. Wadford, J.S. Chen, C.Y. Chiu, CRISPR–Cas12-based detection of SARS-CoV-2, Nat. Biotechnol. 38 (2020) 870–874.

[9] B. Ning, T. Yu, S. Zhang, Z. Huang, D. Tian, Z. Lin, A. Niu, N. Golden, K. Hensley, B. Threeton, C.J. Lyon, X.M. Yin, C.J. Roy, N.S. Saba, J. Rappaport, Q. Wei, T.Y. Hu, A smartphone-read ultrasensitive and quantitative saliva test for COVID-19, Sci. Adv. 7 (2021), eabe3703.

[10] I.A. Mattioli, A. Hassan, O.N. Oliveira, F.N. Crespilho, On the challenges for the diagnosis of SARS-CoV-2 based on a review of current methodologies, ACS Sens. 5 (2020) 3655–3677.

[11] C. Parolo, A. Sena-Torralba, J.F. Bergua, E. Calucho, C. Fuentes-Chust, L. Hu, L. Rivas, R. Álvarez-Diduk, E.P. Nguyen, S. Cinti, D. Quesada-González, A. Merkoçi, Tutorial: design and fabrication of nanoparticle-based lateral-flow immunoassays, Nat. Protoc. 15 (2020) 3788–3816.

[12] M.L. Everitt, A. Tillery, M.G. David, N. Singh, A. Borison, I.M. White, A critical review of point-of-care diagnostic technologies to combat viral pandemics, Anal. Chim. Acta 1146 (2021) 184–199.

[13] R. Paul, E. Ostermann, Q. Wei, Advances in point-of-care nucleic acid extraction technologies for rapid diagnosis of human and plant diseases, Biosens. Bioelectron. 169 (2020) 112592.

[14] T. Notomi, H. Okayama, H. Masubuchi, T. Yonekawa, K. Watanabe, N. Amino, T. Hase, Loop-mediated isothermal amplification of DNA, Nucleic Acids Res. 28 (2000).

[15] H. Thi, C. Thai, M.Q. Le, C.D. Vuong, M. Parida, H. Minekawa, T. Notomi, F. Hasebe, Development and evaluation of a novel loop-mediated isothermal amplification method for rapid detection of severe acute respiratory syndrome coronavirus development and evaluation of a novel loop-mediated isothermal amplification method for rapid detectio, J. Clin. Microbiol. 42 (2004) 1956–1961.

[16] L.L.M. Poon, C.S.W. Leung, K.H. Chan, J.H.C. Lee, K.Y. Yuen, Y. Guan, J.S.M. Peiris, Detection of human influenza A viruses by loop-mediated isothermal amplification, J. Clin. Microbiol. 43 (2005) 427–430.

[17] S.H. Lee, Y.H. Baek, Y.H. Kim, Y.K. Choi, M.S. Song, J.Y. Ahn, One-pot reverse transcriptional loop-mediated isothermal amplification (RT-LAMP) for detecting MERS-CoV, Front. Microbiol. 7 (2017).

[18] R. Lu, X. Wu, Z. Wan, Y. Li, X. Jin, C. Zhang, A novel reverse transcription loop-mediated isothermal amplification method for rapid detection of SARS-CoV-2, Int. J. Mol. Sci. 21 (2020) 2826.

[19] V.L. Dao Thi, K. Herbst, K. Boerner, M. Meurer, L.P.M. Kremer, D. Kirrmaier, A. Freistaedter, D. Papagiannidis, C. Galmozzi, M.L. Stanifer, S. Boulant, S. Klein, P. Chlanda, D. Khalid, I.B. Miranda, P. Schnitzler, H.G. Kräusslich, M. Knop, S. Anders, A colorimetric RT-LAMP assay and LAMP-sequencing for detecting SARS-CoV-2 RNA in clinical samples, Sci. Transl. Med. 12 (2020) 7075.

[20] D.M. Dudley, C.M. Newman, A.M. Weiler, M.D. Ramuta, C.G. Shortreed, A.S. Heffron, M.A. Accola, W.M. Rehrauer, T.C. Friedrich, D.H. O'Connor, Optimizing direct RT-LAMP to detect transmissible SARS-CoV-2 from primary nasopharyngeal swab samples, PLoS One 15 (2020), e0244882.

[21] J.C. Rolando, E. Jue, J.T. Barlow, R.F. Ismagilov, Real-time kinetics and high-resolution melt curves in single-molecule digital LAMP to differentiate and study specific and non-specific amplification, Nucleic Acids Res. 48 (2020) e42.

[22] K. Hsieh, P.L. Mage, A.T. Csordas, M. Eisenstein, H.T. Soh, Simultaneous elimination of carry-over contamination and detection of DNA with uracil-DNA-glycosylase-supplemented loop-mediated isothermal amplification (UDG-LAMP), Chem. Commun. 50 (2014) 3747–3749.

[23] S. Ding, G. Chen, Y. Wei, J. Dong, F. Du, X. Cui, X. Huang, Z. Tang, Sequence-specific and multiplex detection of COVID-19 virus (SARS-CoV-2) using proofreading enzyme-mediated probe cleavage coupled with isothermal amplification, Biosens. Bioelectron. 178 (2021) 113041.

[24] X. Gao, B. Sun, Y. Guan, Pullulan reduces the non-specific amplification of loop-mediated isothermal amplification (LAMP), Anal. Bioanal. Chem. 411 (2019) 1211–1218.

[25] Y. Zhang, N. Odiwuor, J. Xiong, L. Sun, R.O. Nyaruaba, H. Wei, N.A. Tanner, Rapid molecular detection of SARS-CoV-2 (COVID-19) virus RNA using colorimetric LAMP, medRxiv 2 (2020) 2020, 02.26.20028373.

[26] I. Smyrlaki, M. Ekman, A. Lentini, N. Rufino de Sousa, N. Papanicolaou, M. Vondracek, J. Aarum, H. Safari, S. Muradrasoli, A.G. Rothfuchs, J. Albert, B. Högberg, B. Reinius, Massive and rapid COVID-19 testing is feasible by extraction-free SARS-CoV-2 RT-PCR, Nat. Commun. 11 (2020) 4812.

[27] P.E. Vandeventer, K.M. Weigel, J. Salazar, B. Erwin, B. Irvine, R. Doebler, A. Nadim, G.A. Cangelosi, A. Niemz, Mechanical disruption of lysis-resistant bacterial cells by use of a miniature, low-power, disposable device, J. Clin. Microbiol. 49 (2011) 2533–2539.

[28] L. Mautner, C.K. Baillie, H.M. Herold, W. Volkwein, P. Guertler, U. Eberle, N. Ackermann, A. Sing, M. Pavlovic, O. Goerlich, U. Busch, L. Wassill, I. Huber, A. Baiker, Rapid point-of-care detection of SARS-CoV-2 using reverse transcription loop-mediated isothermal amplification (RT-LAMP), Virol. J. 17 (2020) 160.

[29] M.A. Lalli, J.S. Langmade, X. Chen, C.C. Fronick, C.S. Sawyer, L.C. Burcea, M.N. Wilkinson, R.S. Fulton, M. Heinz, W.J. Buchser, R.D. Head, R.D. Mitra, J. Milbrandt, Rapid and extraction-free detection of SARS-CoV-2 from saliva by colorimetric reverse-transcription loop-mediated isothermal amplification, Clin. Chem. 67 (2021) 415–424.

[30] R. Nyaruaba, C. Li, C. Mwaliko, M. Mwau, N. Odiwuor, E. Muturi, C. Muema, J. Xiong, J. Li, J. Yu, H. Wei, Developing multiplex ddPCR assays for SARS-CoV-2 detection based on probe mix and amplitude based multiplexing, Expert Rev. Mol. Diagn. (2021) 1–11.

[31] R.J. Meagher, A. Priye, Y.K. Light, C. Huang, E. Wang, Impact of primer dimers and self-amplifying hairpins on reverse transcription loop-mediated isothermal amplification detection of viral RNA, Analyst 143 (2018) 1924–1933.

[32] Y. Zhang, G. Ren, J. Buss, A.J. Barry, G.C. Patton, N.A. Tanner, Enhancing Colorimetric Loop-Mediated Isothermal Amplification Speed and Sensitivity with Guanidine Chloride, Biotechniques, 2020. btn-2020-0078.

[33] B.A. Rabe, C. Cepko, SARS-CoV-2 detection using isothermal amplification and a rapid, inexpensive protocol for sample inactivation and purification, Proc. Natl. Acad. Sci. Unit. States Am. 117 (2020), 202011221.

[34] D.R. Marinowic, G. Zanirati, F.V.F. Rodrigues, M.V.C. Grahl, A.M. Alcará, D.C. Machado, J.C. Da Costa, A new SYBR Green real-time PCR to detect SARS-CoV-2, Sci. Rep. 11 (2021) 2224.

[35] J. Dong, Q. Xu, C.C. Li, C.Y. Zhang, Single-color multiplexing by the integration of high-resolution melting pattern recognition with loop-mediated isothermal amplification, Chem. Commun. 55 (2019) 2457–2460.

[36] J. Li, X. Hu, X. Wang, J. Yang, L. Zhang, Q. Deng, X. Zhang, Z. Wang, T. Hou, S. Li, A novel One-pot rapid diagnostic technology for COVID-19, Anal. Chim. Acta 1154 (2021) 338310.

[37] H. Zhou, D. Liu, L. Ma, T. Ma, T. Xu, L. Ren, L. Li, S. Xu, A SARS-CoV-2 reference standard quantified by multiple digital PCR platforms for quality assessment of molecular tests, Anal. Chem. 93 (2021) 715–721.

[38] C. Yan, J. Cui, L. Huang, B. Du, L. Chen, G. Xue, S. Li, W. Zhang, L. Zhao, Y. Sun, H. Yao, N. Li, H. Zhao, Y. Feng, S. Liu, Q. Zhang, D. Liu, J. Yuan, Rapid and visual detection of 2019 novel coronavirus (SARS-CoV-2) by a reverse transcription loop-mediated isothermal amplification assay, Clin. Microbiol. Infect. 26 (2020) 773–779.

[39] W.E. Huang, B. Lim, C. Hsu, D. Xiong, W. Wu, Y. Yu, H. Jia, Y. Wang, Y. Zeng, M. Ji, H. Chang, X. Zhang, H. Wang, Z. Cui, RT-LAMP for rapid diagnosis of coronavirus SARS-CoV-2, Microb. Biotechnol. 13 (2020) 950–961.

[40] Y.H. Baek, J. Um, K.J.C. Antigua, J.H. Park, Y. Kim, S. Oh, Y. Il Kim, W.S. Choi, S.G. Kim, J.H. Jeong, B.S. Chin, H.D.G. Nicolas, J.Y. Ahn, K.S. Shin, Y.K. Choi, J.S. Park, M.S. Song, Development of a reverse transcription-loop-mediated isothermal amplification as a rapid early-detection method for novel SARS-CoV-2, Emerg, Microb. Infect. 9 (2020) 1–31.

[41] N.A. Tanner, Y. Zhang, T.C. Evans, Visual detection of isothermal nucleic acid amplification using pH-sensitive dyes, Biotechniques 58 (2015) 59–68.

[42] T.L. Quyen, T.A. Ngo, D.D. Bang, M. Madsen, A. Wolff, Classification of multiple DNA dyes based on inhibition effects on real-time loop-mediated isothermal amplification (LAMP): prospect for point of care setting, Front. Microbiol. 10 (2019).

[43] R.W. Doebler, B. Erwin, A. Hickerson, B. Irvine, D. Woyski, A. Nadim, J.D. Sterling, Continuous-flow, rapid lysis devices for biodefense nucleic acid diagnostic systems, J. Assoc. Lab. Autom. 14 (2009) 119–125.

[44] L.J.A. Beckers, M. Baragona, S. Shulepov, T. Vliegenthart, A.R. Van Doorn, Mechanical cell lysis device, 14th int. Conf. Miniaturized syst. Chem. Life sci. 2010, Micro 1 (2010) 85–87, 2010.

[45] H. Zhu, Z. Fohlerová, J. Pekárek, E. Basova, P. Neužil, Recent advances in lab-on-a-chip technologies for viral diagnosis, Biosens. Bioelectron. 153 (2020) 112041.

[46] E. Di Stasio, R. De Cristofaro, The effect of shear stress on protein conformation: physical forces operating on biochemical systems: the case of von Willebrand factor, Biophys. Chem. 153 (2010) 1–8.

[47] J. Lyu, Y. Wang, C. Ruan, X. Zhang, K. Li, M. Ye, Mechanical stress induced protein precipitation method for drug target screening, Anal. Chim. Acta 1168 (2021) 338612.
[48] P.S. Walsh, D.A. Metzger, R. Higuchi, Chelex 100 as a medium for simple extraction of DNA for PCR-based typing from forensic material, Biotechniques 54 (2013) 134–139.
[49] S. Ding, G. Chen, Y. Wei, J. Dong, F. Du, X. Cui, X. Huang, Z. Tang, Sequence-specific and multiplex detection of COVID-19 virus (SARS-CoV-2) using proofreading enzyme-mediated probe cleavage coupled with isothermal amplification, Biosens. Bioelectron. 178 (2021) 113041.
[50] S. Klein, T.G. Müller, D. Khalid, V. Sonntag-Buck, A.M. Heuser, B. Glass, M. Meurer, I. Morales, A. Schillak, A. Freistaedter, I. Ambiel, S.L. Winter, L. Zimmermann, T. Naumoska, F. Bubeck, D. Kirrmaier, S. Ullrich, I.B. Miranda, S. Anders, D. Grimm, P. Schnitzler, M. Knop, H.G. Kräusslich, V.L.D. Thi, K. Börner, P. Chlanda, SARS-CoV-2 RNA extraction using magnetic beads for rapid large-scale testing by RT-qPCR and RT-LAMP, Viruses 12 (2020).
[51] L. Bokelmann, O. Nickel, T. Maricic, S. Pääbo, M. Meyer, S. Borte, S. Riesenberg, Point-of-care bulk testing for SARS-CoV-2 by combining hybridization capture with improved colorimetric LAMP, Nat. Commun. 12 (2021) 1–8.
[52] B. Guan, K.M. Frank, J.O. Maldonado, M. Beach, E. Pelayo, B.M. Warner, R.B. Hufnagel, Sensitive extraction-free SARS-CoV-2 RNA virus detection using a chelating resin, iScience 24 (2021) 102960.
[53] N. Ben-Assa, R. Naddaf, T. Gefen, T. Capucha, H. Hajjo, N. Mandelbaum, L. Elbaum, P. Rogov, D.A. King, S. Kaplan, A. Rotem, M. Chowers, M. Szwarcwort-Cohen, M. Paul, N. Geva-Zatorsky, Direct on-the-spot detection of SARS-CoV-2 in patients, Exp. Biol. Med. 245 (2020) 1187–1193.
[54] L. Azzi, G. Carcano, F. Gianfagna, P. Grossi, D.D. Gasperina, A. Genoni, M. Fasano, F. Sessa, L. Tettamanti, F. Carinci, V. Maurino, A. Rossi, A. Tagliabue, A. Baj, Saliva is a reliable tool to detect SARS-CoV-2, J. Infect. 81 (2020) e45–e50.
[55] K.G. Rodino, M.J. Espy, S.P. Buckwalter, R.C. Walchak, J.J. Germer, E. Fernholz, A. Boerger, A.N. Schuetz, J.D. Yao, M.J. Binnicker, Evaluation of saline, phosphate-buffered saline, and minimum essential medium as potential alternatives to viral transport media for SARS-CoV-2 testing, J. Clin. Microbiol. 58 (2020).
[56] A. Singanayagam, M. Patel, A. Charlett, J. Lopez Bernal, V. Saliba, J. Ellis, S. Ladhani, M. Zambon, R. Gopal, Duration of infectiousness and correlation with RT-PCR cycle threshold values in cases of COVID-19, England, January to May 2020, Euro Surveill. 25 (2020) 2001483.